



# Antipodoplanin antibody enhances the antitumor effects of CTLA-4 blockade against malignant mesothelioma by natural killer cells

Hiroto Yoneda<sup>1</sup> | Atsushi Mitsuhashi<sup>1</sup> | Aito Yoshida<sup>2</sup> | Hirokazu Ogino<sup>1</sup> | Satoshi Itakura<sup>2</sup> | Na Thi Nguyen<sup>1</sup> | Hiroshi Nokihara<sup>1</sup> | Seidai Sato<sup>1</sup> | Tsutomu Shinohara<sup>3</sup> | Masaki Hanibuchi<sup>4</sup> | Shinji Abe<sup>2</sup> | Mika K. Kaneko<sup>5</sup> | Yukinari Kato<sup>5</sup>  | Yasuhiko Nishioka<sup>1,6</sup> 

<sup>1</sup>Department of Respiratory Medicine and Rheumatology, Tokushima University, Tokushima, Japan

<sup>2</sup>Department of Clinical Pharmacy Practice Pedagogy, Tokushima University, Tokushima, Japan

<sup>3</sup>Department of Community Medicine for Respiriology, Tokushima University, Tokushima, Japan

<sup>4</sup>Department of Community Medicine for Respiriology, Hematology and Metabolism, Graduate School of Biomedical Sciences, Tokushima University, Tokushima, Japan

<sup>5</sup>Department of Antibody Drug Development, Tohoku University Graduate School of Medicine, Sendai, Japan

<sup>6</sup>Department of Community Medicine for Rheumatology, Graduate School of Biomedical Sciences, Tokushima University, Tokushima, Japan

## Correspondence

Yasuhiko Nishioka, Department of Respiratory Medicine and Rheumatology, Tokushima University, 3-18-15 Kuramoto-cho, Tokushima, Tokushima 770-8503, Japan.

Email: [yasuhiko@tokushima-u.ac.jp](mailto:yasuhiko@tokushima-u.ac.jp)

## Funding information

Japan Agency for Medical Research and Development, Grant/Award Number: JP21am0101078 and JP22ama121008; Japan Society for the Promotion of Science, Grant/Award Number: 19H03668, 20K07197 and 20K17216

## Abstract

Combination immunotherapy with multiple immune checkpoint inhibitors (ICIs) has been approved for various types of malignancies, including malignant pleural mesothelioma (MPM). Podoplanin (PDPN), a transmembrane sialomucin-like glycoprotein, has been investigated as a diagnostic marker and therapeutic target for MPM. We previously generated and developed a PDPN-targeting Ab reagent with high Ab-dependent cellular cytotoxicity (ADCC) and complement-dependent cytotoxicity (CDC). However, the effects of anti-PDPN Abs on various tumor-infiltrating immune cells and their synergistic effects with ICIs have remained unclear. In the present study, we established a novel rat-mouse chimeric anti-mouse PDPN IgG<sub>2a</sub> mAb (PMab-1-mG<sub>2a</sub>) and its core-fucose-deficient Ab (PMab-1-mG<sub>2a</sub>-f) to address these limitations. We identified the ADCC and CDC activity of PMab-1-mG<sub>2a</sub>-f against the PDPN-expressing mesothelioma cell line AB1-HA. The antitumor effect of monotherapy with PMab-1-mG<sub>2a</sub>-f was not sufficient to overcome tumor progression in AB1-HA-bearing immunocompetent mice. However, PMab-1-mG<sub>2a</sub>-f enhanced the antitumor effects of CTLA-4 blockade. Combination therapy with anti-PDPN Ab and anti-CTLA-4 Ab increased tumor-infiltrating natural killer (NK) cells. The depletion

**Abbreviations:** ADCC, antibody-dependent cellular cytotoxicity; CDC, complement-dependent cytotoxicity; CTLA-4, CTL-associated antigen 4; HER2, human epidermal growth factor receptor 2; ICI, immune checkpoint inhibitor; IL-2R $\beta$ , interleukin-2 receptor  $\beta$ -chain; MPM, malignant pleural mesothelioma; NK, natural killer; OS, overall survival; PD-1, programmed death 1; PD-L1, programmed death ligand 1; PDPN, podoplanin; T<sub>reg</sub>, regulatory T cell.

This is an open access article under the terms of the [Creative Commons Attribution-NonCommercial-NoDerivs](https://creativecommons.org/licenses/by-nc-nd/4.0/) License, which permits use and distribution in any medium, provided the original work is properly cited, the use is non-commercial and no modifications or adaptations are made.

© 2023 The Authors. *Cancer Science* published by John Wiley & Sons Australia, Ltd on behalf of Japanese Cancer Association.

of NK cells inhibited the synergistic effects of PMab-1-mG<sub>2a</sub>-f and CTLA-4 blockade in vivo. These findings indicated the essential role of NK cells in novel combination immunotherapy targeting PDPN and shed light on the therapeutic strategy in advanced MPM.

#### KEYWORDS

CTLA-4, immune checkpoint inhibitor, malignant pleural mesothelioma, NK cell, podoplanin

## 1 | INTRODUCTION

Malignant pleural mesothelioma is an aggressive malignant tumor mainly caused by environmental asbestos exposure.<sup>1-3</sup> The prognosis of MPM is extremely poor because of its poor response to cytotoxic chemotherapy and the difficulty making an early diagnosis.

A recent study revealed that platinum-based chemotherapy with pemetrexed prolonged the OS of advanced MPM patients compared with platinum monotherapy (12.1 vs. 9.3 months).<sup>4</sup> However, because of its insufficient efficacy and the lack of validated second-line therapy, novel therapeutic strategies for MPM have long been sought.

Immune checkpoint inhibitors targeting PD-1, PD-L1, and CTLA-4 have shown clinical benefit in various types of malignancies.<sup>5-7</sup> The phase III CheckMate743 trial showed that combination immunotherapy with an anti-PD-1 Ab (nivolumab) and anti-CTLA-4 Ab (ipilimumab) results in superior improvements in the OS in unresectable MPM cases compared with platinum-based chemotherapy with pemetrexed (18.1 vs. 14.1 months).<sup>8</sup> Combination immunotherapy has shed new light on therapeutic strategies for unresectable MPM. Thus, the detection of novel therapeutic targets in the tumor immune microenvironment is required to overcome the poor prognosis of MPM.

Podoplanin, a transmembrane sialomucin-like glycoprotein, was first identified as the regulatory molecule of podocyte morphology in the kidney.<sup>9</sup> The expression of PDPN was also detected in lymphatic endothelial cells as a marker of lymphangiogenesis.<sup>10</sup> The PDPN expression has been investigated as a cell surface marker for various types of malignancies as well, including oral cancers, colorectal cancers, squamous lung carcinoma, and MPM.<sup>11-14</sup> Therefore, PDPN has potential utility as a diagnostic biomarker and tumor-associated antigen for immunotherapy in MPM.

Several therapeutic Abs targeting tumor-associated antigens have been approved for various malignancies, such as rituximab (anti-CD20 Ab) and trastuzumab (anti-HER2 Ab).<sup>15,16</sup> These Abs have been known to exert tumor-killing effects through ADCC and CDC.<sup>17</sup> In our previous studies, we generated a specific Ab targeting PDPN and investigated its antitumor effects in vitro and in preclinical models. A rat anti-human PDPN mAb, NZ-1,<sup>18</sup> and a rat-human chimeric anti-human PDPN Ab, NZ-8<sup>19</sup> and NZ-12,<sup>20</sup> showed high ADCC and CDC activity and enhanced the antitumor effects of NK

cells in human MPM cell-bearing SCID mice. In a previous study, we mainly focused on the ADCC activity of the anti-PDPN Ab by binding the Fc receptor in NK cells. However, in the actual tumor immune microenvironment, immunotherapy targets multiple immune cells, including T cells, B cells, NK cells, and T<sub>regs</sub>. To evaluate the antitumor effects of anti-PDPN Abs and their interactions with known immunotherapies, including ICIs, a preclinical study in immunocompetent conditions is needed.

We generated a novel rat-mouse chimeric anti-mouse PDPN IgG<sub>2a</sub> mAb (PMab-1-mG<sub>2a</sub>) to detect the expression of PDPN in mouse tumor cells. In addition, we also produced a core-fucose-deficient Ab to improve ADCC activity (PMab-1-mG<sub>2a</sub>-f). In the present study, we investigated the antitumor effects of an anti-mouse PDPN Ab under immunocompetent conditions and its influence on various immune cells in the tumor microenvironment. Furthermore, the synergistic effects of anti-PDPN Abs with ICIs, such as PD-1 blockade and CTLA-4 blockade, were examined to develop a novel combination immunotherapy for MPM.

## 2 | MATERIALS AND METHODS

### 2.1 | Cell lines

The mouse malignant mesothelioma cell line AB1-HA, a transfectant with the gene encoding influenza HA into AB1 cells and the mouse malignant mesothelioma cell line AC29 were purchased from Public Health England. The mouse lung cancer cell line LLC was purchased from ATCC. Mouse melanoma cell line B16 was kindly provided by Dr. IJ Fidler (MD Anderson Cancer Center). The mouse fibrosarcoma cell line MCA205 and mouse colon carcinoma cell line MC38 were generously provided by Dr. SA Rosenberg (National Cancer Institute, National Institutes of Health). AB1-HA was maintained in DMEM supplemented with 10% heat-inactivated FBS, penicillin (100 U/mL), and streptomycin (50 µg/mL). The other cell lines were maintained in RPMI-1640. All cells were cultured at 37°C in a humidified atmosphere of 5% CO<sub>2</sub> in air.

### 2.2 | Reagents

Anti-mouse PD-1 (clone RMP1-14) and anti-mouse CTLA-4 (clone 4F10) Abs were purchased from BioXCell. Isotype control IgG

(rat IgG<sub>1</sub>, rat IgG<sub>2a</sub>, and hamster IgG) were also purchased from BioXCell. PMab-1, a rat anti-mouse PDPN mAb, was developed as previously described.<sup>21</sup> For the generation of rat-mouse chimeric anti-mouse PDPN IgG<sub>2a</sub> mAb (PMab-1-mG<sub>2a</sub>), appropriate V<sub>H</sub> cDNA of rat PMab-1 was subcloned into pFUSE-CHIGmG<sub>2a</sub> (InvivoGen) and appropriate V<sub>L</sub> cDNA of rat PMab-1 and C<sub>L</sub> of mouse kappa chain were subcloned into pCAG-Neo vector (FUJIFILM Wako Pure Chemical Corporation), respectively. Antibody expression vectors were transfected into ExpiCHO-S (Thermo Fisher Scientific Inc.) using the ExpiCHO Expression System (Thermo Fisher Scientific Inc.). The core fucose-deficient type of PMab-1-mG<sub>2a</sub> (PMab-1-mG<sub>2a</sub>-f) was produced by transfecting them into FUT8-deficient ExpiCHO-S cells (BINDS-09).<sup>22</sup> An anti-mouse IL-2R $\beta$  mAb, TM- $\beta$ 1 (IgG<sub>2b</sub>), was a gift from Drs. Masayuki Miyasaka and Toshio Tanaka (Osaka University, Osaka, Japan). Anti-mouse CD4 (clone GK1.5) and anti-mouse CD8 (clone 2.43) Abs were purchased from BioXCell.

## 2.3 | Animals

Six-week-old male BALB/c mice, C57BL/6J mice, and C.B-17 SCID mice were obtained from Charles River Japan Inc. All experiments were carried out in accordance with the guidelines established by the Tokushima University Committee on Animal Care and Use. At the end of each in vivo experiment, the mice were anesthetized with isoflurane and euthanized humanely by cutting the subclavian artery. All experimental protocols were reviewed and approved by the animal research committee of The University of Tokushima.

## 2.4 | In vivo s.c. implantation models of mouse tumor cells

AB1-HA cells or LLC cells ( $1.0 \times 10^6$  cells per mouse) suspended in 0.1 mL PBS were s.c. inoculated to the right flank of BALB/c or C57BL/6J mice, respectively. The tumor size was measured using vernier calipers twice a week, where volume =  $\frac{ab^2}{2}$  (a, long diameter; b, short diameter). To evaluate the effects of anti-mouse PDPN Ab, the mice were treated with PMab-1-mG<sub>2a</sub>-f (50 or 100 or 500  $\mu$ g per mouse) twice a week. To determine the synergistic effects of anti-PDPN Ab with PD-1 blockade or CTLA-4 blockade on tumor growth, the mice were treated twice a week with PMab-1-mG<sub>2a</sub>-f (50  $\mu$ g per mouse), anti-PD-1 Ab (200  $\mu$ g per mouse), anti-CTLA-4 Ab (5  $\mu$ g per mouse), or isotype control IgG by i.p. injection from day 7 until they became moribund. To deplete NK cells, the mice were pretreated with anti-mouse IL-2R $\beta$  Ab 4 days after tumor inoculation. To deplete CD4<sup>+</sup> T cells or CD8<sup>+</sup> T cells, the mice were treated with anti-mouse CD4 or CD8 Abs (200  $\mu$ g per mouse) twice a week from 4 days after tumor inoculation. The mice were killed humanely, and the tumors were resected for further analyses on days 21.

## 2.5 | Immunofluorescence of mouse tumor tissues

The excised tumor tissues from the model mice were placed into OCT compound (Sakura Finetechnical Co.) and snap-frozen. Frozen tissue sections (8  $\mu$ m thick) were fixed with 4% paraformaldehyde solution in PBS and used for the identification of NK cells, CD8<sup>+</sup> and CD4<sup>+</sup> T cells, and T<sub>reg</sub>s using a goat anti-mouse NKp46 (1:100; R&D Systems), rat anti-CD8a mAb (1:150, 53-6.7; BD Pharmingen), rat anti-mouse CD4 (1:150, H129.19; BD Pharmingen), and a rabbit anti-Foxp3 polyclonal Ab (1:400 dilution; Novus Biologicals), respectively. To identify NKT cells, rat anti-mouse CD3 (1:150, H129.19; BD Pharmingen), and a rabbit anti-mouse CD49b polyclonal Ab (1:150 dilution, Thermo Fisher Scientific Inc.) were used. Alexa488- and Alexa594-labeled secondary Abs (1:250; Thermo Fisher Scientific Inc.) were used for immunofluorescent detection. Nuclei were counter-stained with DAPI (blue). In each slide, the number of positive cells was counted under a fluorescent microscope at  $\times 200$  magnification. These images were acquired using a BX61 fluorescence light microscope (Olympus).

## 2.6 | Flow cytometry

To examine the surface expression of PDPN in mouse tumor cell lines, tumor cells were incubated with PMab-1-mG<sub>2a</sub> or isotype control (1  $\mu$ g/mL) for 30 min. Cells were washed with PBS and incubated for 30 min with FITC-conjugated goat F(ab')<sub>2</sub> fragment anti-rat IgG (H+L) Ab (Beckman Coulter). AB1-HA tumor tissue was cut into small pieces with scissors and digested by digestion buffer consisting of 1 mg/mL BSA (Sigma-Aldrich), 1 mg/mL collagenase IV (Thermo Fisher Scientific Inc.), and 100  $\mu$ g/mL DNase I (Roche) in DMEM for 40 min of incubation at 37°C, followed by passaging through a 100  $\mu$ m cell strainer. The cells were incubated with FcR blocking reagent (BD Biosciences). To examine the surface expression of CTLA-4 and PD-1 in mouse tumor-infiltrating immune cells, tumor tissue-derived cells were stained with FITC-conjugated anti-NKp46 (BioLegend), FITC-conjugated anti-CD8a (BD Biosciences), FITC-conjugated anti-CD4 (BD Biosciences), FITC-conjugated anti-F4/80 (BioLegend), PE-Cy7-conjugated anti-CTLA-4 (BioLegend), and PE-Cy7-conjugated anti-PD-1 (BioLegend). The stained cells were analyzed by flow cytometry using a BD LSRFortessa (BD Biosciences) for acquisition and the FlowJo software program (Treestar Inc.) for the analysis.

## 2.7 | Preparation of effector cells

Mouse splenocytes were harvested from C.B-17 SCID mice spleens. Spleens were homogenized in RPMI-1640 and centrifuged. To deplete red blood cells, the cell pellet was suspended in red blood cell lysis buffer (Sigma-Aldrich). After washing and resuspension in RPMI-1640, splenocytes were used as effector cells.

## 2.8 | Antibody-dependent cellular cytotoxicity

Antibody-dependent cellular cytotoxicity was determined using  $^{51}\text{Cr}$  release assays. Target cells (AB1-HA or LLC) were incubated with  $^{51}\text{Cr}$ -sodium chromate (3.7 MBq) at 37°C for 1 h. After washing with RPMI-1640 three times,  $^{51}\text{Cr}$ -labeled target cells were placed in triplicate in 96-well plates. Effector cells and anti-mouse PDPN Abs (PMab-1-mG<sub>2a</sub> or PMab-1-mG<sub>2a</sub>-f, 10 µg/mL) or control IgG were added to the plates (effector/target ratio 100). After 18 h of incubation,  $^{51}\text{Cr}$  release of the supernatant from each well (100 µL) was measured using a gamma counter (PerkinElmer). Percent of cytotoxicity was calculated using the following formula: % specific lysis =  $(E - S)/(M - S) \times 100$ , where E is the release in the test sample, S is the spontaneous release, and M is the maximum release.

## 2.9 | Complement-dependent cytotoxicity

Complement-dependent cytotoxicity was evaluated by  $^{51}\text{Cr}$  release assay. Target cells were incubated with  $^{51}\text{Cr}$ -sodium chromate (3.7 MBq) for 1 h at 37°C. Following this, cells were washed in RPMI-1640. The  $^{51}\text{Cr}$ -labeled cells were incubated with baby rabbit complement (dilution of 1:64) (Cedarlane) and 10 µg/mL Abs for 6 h in 96-well plates. After incubation, the supernatant, including  $^{51}\text{Cr}$ , was

measured using a gamma counter. Percent cytotoxicity was calculated as described above.

## 2.10 | Statistical analyses

The data are presented as the mean  $\pm$  SE of the mean. The statistical analyses were carried out using Student's *t*-test for unpaired samples, the Mann-Whitney *U*-test or a one-way ANOVA, followed by Tukey's multiple comparison post-hoc test, as appropriate. Values of  $p < 0.05$  were considered to be statistically significant.

# 3 | RESULTS

## 3.1 | Evaluating the activity of anti-mouse PDPN Abs against mouse MPM cell lines

Initially, we investigated the expression of PDPN in mouse tumor cell lines using PMab-1-mG<sub>2a</sub> in flow cytometry (Figure 1A). High PDPN expression was identified in the cell membrane of the mouse mesothelioma cell line AB1-HA, colon cancer cell line MC38, and melanoma cell line B16. To evaluate the antitumor effects of the anti-mouse PDPN Ab against MPM, we next evaluated the ADCC (Figure 1B) and CDC (Figure 1C) activities of PMab-1-mG<sub>2a</sub> and its

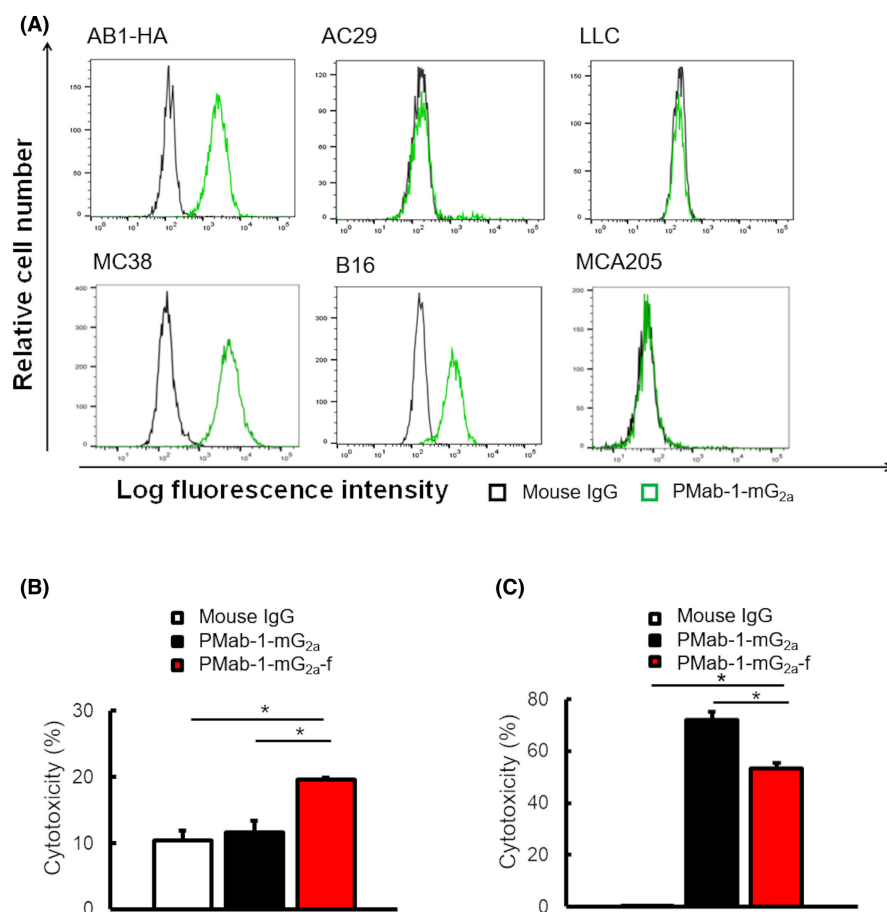


**FIGURE 1** Functional analysis of the rat-mouse chimeric anti-mouse podoplanin (PDPN) Ab. (A) Detection of PDPN on the cell surface of mouse tumor cell lines by PMab-1-mG<sub>2a</sub>. (B) Evaluation of the Ab-dependent cellular cytotoxicity activity of PMab-1-mG<sub>2a</sub> and PMab-1-mG<sub>2a</sub>-f using splenocytes of SCID mice against AB1-HA by an 18 h  $^{51}\text{Cr}$  release assay in the presence of Ab (10 µg/mL; effector/target ratio 100). (C) Evaluation of the complement-dependent cytotoxicity activity of PMab-1-mG<sub>2a</sub> and PMab-1-mG<sub>2a</sub>-f using baby rabbit complement against AB1-HA by a 6 h  $^{51}\text{Cr}$  release assay in the presence of Ab (10 µg/mL; dilution ratio 64). Data are shown as the mean  $\pm$  SEM. \* $p < 0.05$  by a one-way ANOVA.

core-fucose-deficient Ab, PMab-1-mG<sub>2a</sub>-f. Splenocytes from SCID mice were used as effector cells to evaluate the NK cell-dependent ADCC activity of the anti-PDPN Ab. Several studies have shown that core-fucose-deficient Abs demonstrate high ADCC activities.<sup>23,24</sup> In the present study, PMab-1-mG<sub>2a</sub> did not show mouse splenocyte-dependent ADCC activity against PDPN-expressing mesothelioma cells but did demonstrate high CDC activity in vitro. In contrast, core-fucose-deficient PMab-1-mG<sub>2a</sub>-f enhanced the tumor killing capability of mouse splenocytes by ADCC activity (Figure 1B). The ADCC (Figure S1A) and CDC (Figure S1B) activity of anti-PDPN Abs against PDPN-negative tumor cells (LLC) were also evaluated. The tumor killing capability of PMab-1-mG<sub>2a</sub> and PMab-1-mG<sub>2a</sub>-f against PDPN<sup>−</sup> tumors through ADCC or CDC was extremely weak. These results indicated that PMab-1-mG<sub>2a</sub>-f exerted antitumor effects against PDPN<sup>+</sup> MPM through both ADCC and CDC activity.

### 3.2 | Antitumor effects of anti-mouse PDPN Ab in mesothelioma-bearing immunocompetent mice

To determine the antitumor effects of the anti-PDPN Ab on tumor-infiltrating immune cells, we treated AB1-HA-bearing BALB/c mice with PMab-1-mG<sub>2a</sub>-f (Figure 2A,B). The lower amount of PMab-1-mG<sub>2a</sub>-f (50 µg) tended to suppress tumor progression in vivo, whereas higher concentrations (100 µg or 500 µg) failed to demonstrate antitumor effects. In contrast, PMab-1-mG<sub>2a</sub>-f (50 µg) did not show antitumor effects against PDPN<sup>−</sup> LLC tumor tissue in vivo (Figure S1C). We also investigated the effects of PMab-1-mG<sub>2a</sub>-f on tumor immune microenvironment cells by immunohistochemical analysis (Figure 2C–H). The number of NKp46<sup>+</sup> NK cells was slightly increased by treatment with PMab-1-mG<sub>2a</sub>-f in PDPN<sup>+</sup> AB1-HA tumor tissue, while CD8<sup>+</sup> or CD4<sup>+</sup> T lymphocytes did not accumulate. These results suggested the potential of PMab-1-mG<sub>2a</sub>-f to enhance the tumor-killing capacity of NK cells. However, monotherapy with PMab-1-mG<sub>2a</sub>-f seemed to be insufficient for definitive treatment in MPM-bearing mice.

### 3.3 | Synergistic effects of anti-PDPN Ab and CTLA-4 blockade in mesothelioma-bearing mice

Considering the superior clinical outcome of combination immunotherapy in MPM patients,<sup>8</sup> we next focused on combination therapy with PMab-1-mG<sub>2a</sub>-f and ICIs. AB1-HA tumor-bearing mice were treated with PMab-1-mG<sub>2a</sub>-f and ICIs: CTLA-4 blockade (Figure 3A) and PD-1 blockade (Figure 3B). Interestingly, combination therapy with anti-PDPN Ab and anti-CTLA-4 Ab significantly suppressed tumor progression, whereas the antitumor effects of each monotherapy were limited (Figure 3A). In contrast, PMab-1-mG<sub>2a</sub>-f did not reinforce the antitumor effects of anti-PD-1 Ab in AB1-HA tumor-bearing mice (Figure 3B).

To investigate the mechanisms by which the anti-PDPN Ab improved the responses to CTLA-4 blockade, an

immunohistochemical analysis of tumor-infiltrating NK cells (Figure 3C), CD8 T cells (Figure 3D), and CD4 T cells (Figure 3E) was undertaken in each group. CTLA-4 is known to dominate the functions of various immune cells, including T cells, B cells, antigen-presenting cells, and NK cells.<sup>25,26</sup> Consistent with recent studies, CTLA-4 blockade significantly increased tumor-infiltrating NK cells, NKT cells, CD8 T cells, and CD4 T cells (Figures 3F–H and S2A). In addition, combination therapy with PMab-1-mG<sub>2a</sub>-f and CTLA-4 blockade indicated the further accumulation of NK cells and NKT cells in AB1-HA tumor tissue (Figures 3F and S2B). However, the anti-PDPN Ab did not enhance the effects of CTLA-4 blockade on tumor-infiltrating CD8 and CD4 T cells (Figure 3G,H). To examine the target of combined therapy with anti-PDPN Ab and ICIs, the cell surface expression of CTLA-4 and PD-1 in mouse tumor-infiltrating immune cells (Figure S3). The flow cytometry analysis revealed that some populations of tumor-infiltrating NK cells and macrophages expressed CTLA-4, while the majority of T cells did not. Natural killer cells and macrophages were known to mediate ADCC because of FcγRIII (CD16) expression.<sup>15–17</sup> In contrast, the expression of PD-1 was observed in various tumor-infiltrating immune cells, especially in CD4<sup>+</sup> T cells.

Given these findings, we focused on NK cells mediating ADCC as the key therapeutic targets for combination immunotherapy with anti-PDPN Ab and anti-CTLA-4 Ab.

### 3.4 | Natural killer cell dependency in the synergistic effects of anti-PDPN Ab and anti-CTLA-4 Ab

To determine whether or not the synergistic antitumor effects of PMab-1-mG<sub>2a</sub>-f and CTLA-4 blockade required tumor-infiltrating NK cells, we depleted NK cells by treatment with an anti-IL-2Rβ Ab (TMβ-1), as described in previous studies (Figure 4A).<sup>27,28</sup> Pretreatment with TMβ-1 inhibited the antitumor effects of combined immunotherapy with PMab-1-mG<sub>2a</sub>-f and CTLA-4 blockade in AB1-HA tumor-bearing mice (Figure 4B). Considering the possibility that TMβ-1 influenced not only tumor-infiltrating NK cells but also T cells, an immunohistochemical analysis was carried out in AB1-HA tumor tissue (Figure 4C–E). The NK cells accumulated by the combined therapy were notably eliminated by TMβ-1 (Figure 4F), whereas a very slight reduction in tumor-infiltrating CD8 T cells or CD4 T cells was observed (Figure 4G,H). Anti-CTLA-4 Abs have been known to increase or decrease tumor-infiltrating CTLA-4<sup>+</sup> T<sub>reg</sub>s, depending on the ADCC activity.<sup>29–31</sup> In the present study, CTLA-4 blockade treatment increased tumor-infiltrating T<sub>reg</sub>s, consistent with a recent study that used the same clone (Figure S4).<sup>29</sup> Recent studies have also revealed that T<sub>reg</sub>s express IL-2Rβ.<sup>32</sup> TMβ-1 significantly decreased tumor-infiltrating T<sub>reg</sub>s in our preclinical model. However, the antitumor effects of combined immunotherapy with an anti-PDPN Ab and CTLA-4 blockade were inhibited by TMβ-1, despite a reduction in T<sub>reg</sub>s (Figure S4). To evaluate the importance of T cells in the antitumor effects of combined immunotherapy with anti-PDPN



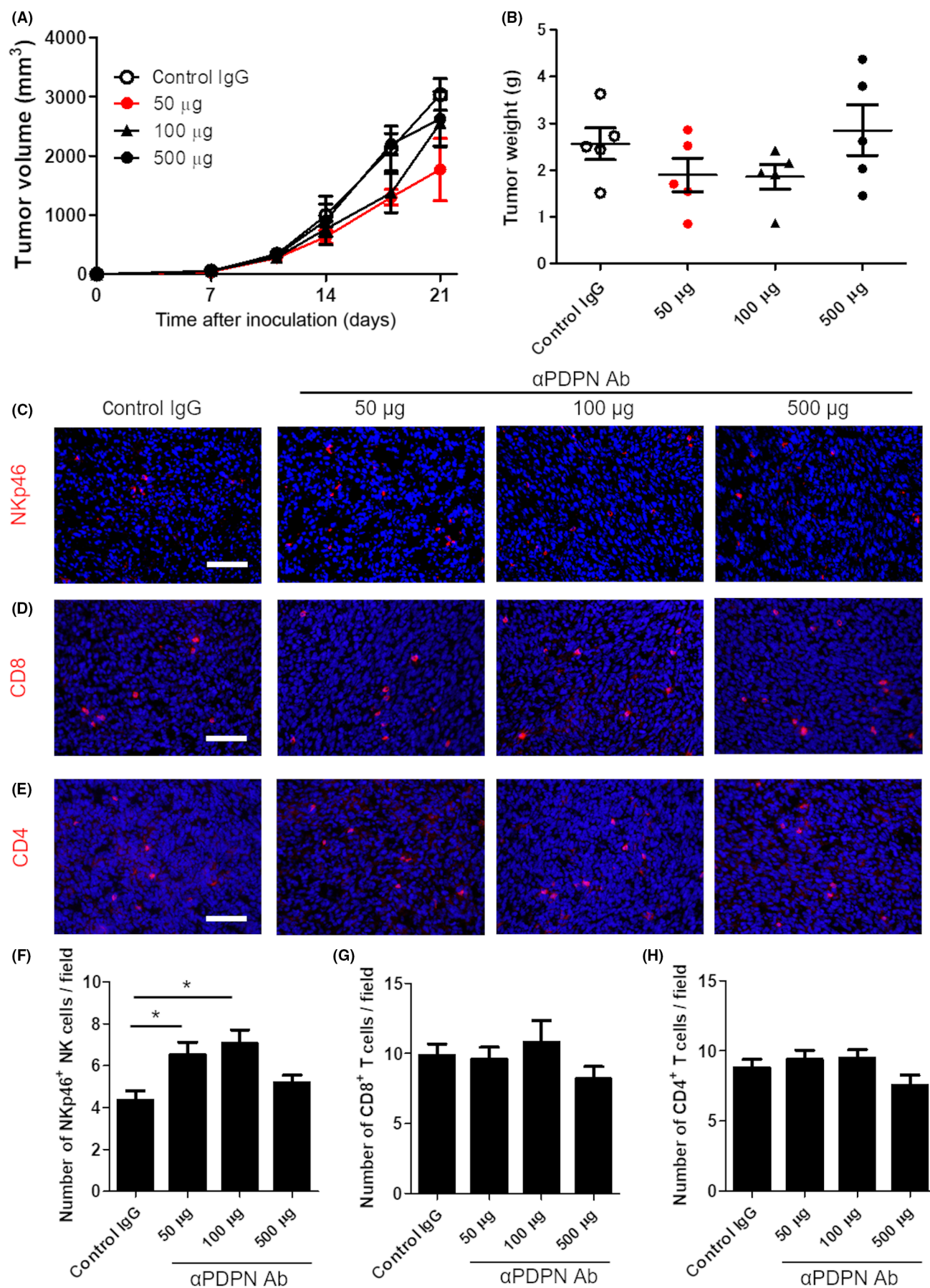


**FIGURE 2** Antitumor effects of monotherapy with core-fucose-deficient rat-mouse chimeric anti-mouse podoplanin (PDPN) Ab in immunocompetent mice. (A, B) Evaluation of the (A) tumor volume and (B) tumor weight of AB1-HA tumor-bearing BALB/c mice treated with PMab-1-mG<sub>2a</sub>-f (50, 100, and 500 µg per mouse) beginning 7 days after tumor cell injection. (C–F) Representative images of sections from AB1-HA tumors stained for (C) natural killer (NK) cells, (D) CD8 T cells, and (E) CD4 T cells. Tumors were harvested at day 21 from each group studied in (A). Scale bar, 200 µm. (F–H) Quantitative evaluation of the total number of (F) NK cells, (G) CD8 T cells, and (H) CD4 T cells in the tumors of mice (*n* = 15 fields per group) is shown in (A). Data are shown as the mean ± SEM. \**p* < 0.05 by a one-way ANOVA.

Ab and CTLA-4 Ab, we also depleted T cells by the administration of anti-CD4 Ab or anti-CD8 T cells (Figure S5). Despite the depletion of T cells, the combination therapy with anti-PDPN Ab and CTLA-4 Ab suppressed mouse tumor progression.

Taken together, these findings suggest that NK cells play pivotal roles in combined immunotherapy with anti-PDPN Abs and anti-CTLA-4 Abs.

## 4 | DISCUSSION

In the present study, we evaluated the efficacy of anti-PDPN Abs in immunocompetent conditions for the first time. Furthermore, we discovered the synergistic antitumor effects of anti-PDPN Ab and anti-CTLA-4 Ab through NK cell-dependent mechanisms.

We previously investigated the antitumor effects of an anti-human PDPN Ab in human MPM cell-bearing SCID mice.<sup>18–20</sup> Previous studies focused on NK cells as the key effector cells because NK cells showed high and specific cytotoxicity against PDPN-expressing tumors treated with anti-PDPN Abs *in vitro*. Combination therapy with peritumoral implantation of NK cells and anti-human PDPN Ab significantly suppressed tumor progression in human MPM-bearing SCID mice, whereas monotherapy with each anti-PDPN Ab did not show an antitumor effect.

These previous studies suggested the potential utility of anti-PDPN Abs as novel immunotherapies against unresectable MPM. However, some limitations to the clinical application of anti-PDPN Abs remained. First, the implantation of human or rat NK cells extracted from peripheral blood or spleen was required to evaluate the antitumor effects of NZ-1, NZ-8, and NZ-12 *in vivo*, as mouse NK cells are known to be insufficient as effector cells of ADCC activities in these anti-PDPN Abs. This limitation made it difficult to evaluate the effects of anti-PDPN Abs on tumor-infiltrating, host-derived NK cells. Second, we inoculated human MPM cells in SCID mice to investigate the affinity and antitumor effects of anti-human PDPN Abs in previous studies. The effects of anti-PDPN Abs on the complicated tumor immune microenvironment, including T cells and B cells, are thus unclear. In the present study, we established the novel rat-mouse chimeric anti-mouse PDPN Ab PMab-1-mG<sub>2a</sub> to overcome these limitations.

In the present study, PMab-1-mG<sub>2a</sub>-f increased tumor-infiltrating NK cells while T cells were not affected (Figure 2). We consider that ADCC mediated by anti-PDPN Ab induced the localization of NK cells in PDPN<sup>+</sup> tumors. Natural killer cells, NKT cells and macrophages were reported to play the pivotal role in ADCC by expressing CD16. Recent reports revealed that Ab drugs targeting HER2 or

epidermal growth factor receptor reinforced the antitumor effects of other immunotherapy and enhanced the accumulation of NK cells in tumor foci.<sup>33,34</sup> Ramamoorthi et al. elucidated that tumor-killing effects of anti-HER2 Ab required CD16 expression in the tumor microenvironment.<sup>34</sup> According to this evidence, we emphasized the ADCC activity in the antitumor effects and the localization of NK cells in tumor by treatment with anti-PDPN Ab. The detailed molecular mechanisms behind ADCC activity-enhanced NK cell accumulation are still unclear and under analysis. The elucidation of the mechanisms is required to develop novel combination immunotherapy with ICI.

Cytotoxicity assays with mouse splenocytes revealed the ADCC and CDC activities of PMab-1-mG<sub>2a</sub> against PDPN-expressing mesothelioma cells. However, monotherapy with PMab-1-mG<sub>2a</sub> showed limited therapeutic effects in mesothelioma-bearing immunocompetent mice, while tumor-infiltrating NK cells were increased. To explain these conflicting results, we focused on the immune checkpoint molecules in tumor-infiltrating NK cells. Natural killer cells are known to express various immune checkpoint molecules, including PD-1, TIGIT, NKG2A, and CTLA-4.<sup>35,36</sup> Of these, the effects of the PD-1/PD-L1 axis and CTLA-4 on tumor-infiltrating NK cells cannot be ignored, given the clinical outcomes of the CheckMate743 trial.<sup>8</sup> Stojanovic et al. showed that IL-2-activated or tumor-infiltrating mouse NK cells expressed CTLA-4, while splenic NK cells did not.<sup>37</sup> CTLA-4 expression in NK cells has been reported to suppress  $\gamma$ -interferon production in response to mature dendritic cells.<sup>37</sup> The efficacy of CTLA-4 blockade on tumor-infiltrating NK cells was therefore investigated in recent studies.<sup>38,39</sup> Davis-Marcisak et al. revealed the Fc receptor-independent binding of anti-CTLA-4 Ab and cell surface CTLA-4 in NK cells.<sup>38</sup> Furthermore, the NK cell activation signature was correlated with an improved overall survival of advanced melanoma patients treated with ipilimumab. Consistent with these recent studies, our preclinical model revealed the synergistic antitumor effects of combined immunotherapy with anti-CTLA-4 Ab and anti-PDPN Ab and its dependency on NK cells.

In our preclinical model, PMab-1-mG<sub>2a</sub> did not enhance the antitumor effects of PD-1 blockade, in contrast to CTLA-4 blockade. Wagner et al. showed that PD-1-deficient NK cells have less capability to migrate and kill tumor cells *in vivo* than WT.<sup>40</sup> They also revealed the cis-binding of PD-1 and PD-L1 on tumor-infiltrating NK cells. This unique function of the PD-1/PD-L1 axis on NK cells partially explains the poor sensitivity to combined therapy with anti-PD-1 Ab and anti-PDPN Ab.

In the present study, the antitumor effects and the accumulation of NK cells by PMab-1-mG<sub>2a</sub>-f were observed only in low concentration (Figure 2). We considered it is due to the prozone

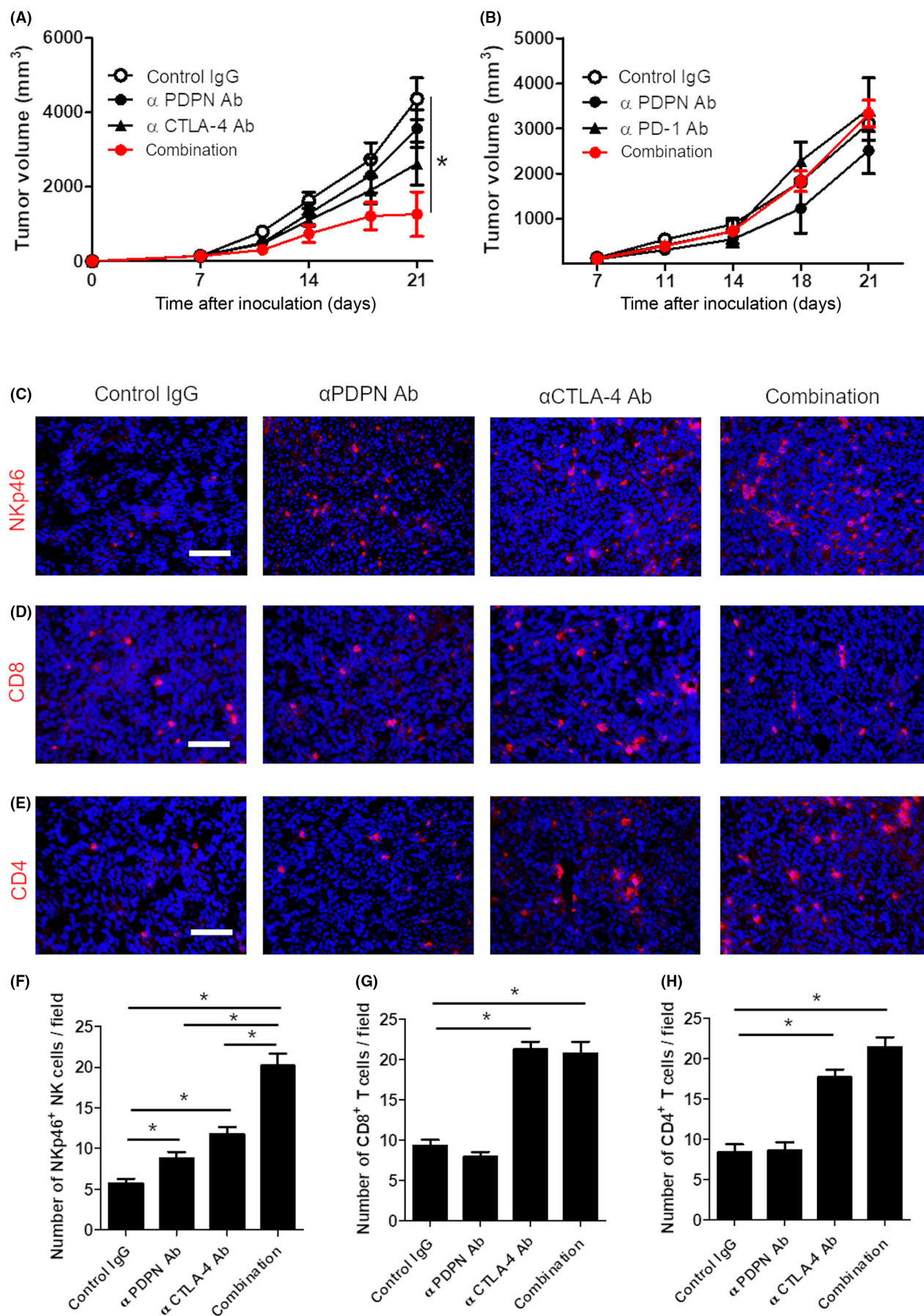




**FIGURE 3** Synergistic effects of anti-podoplanin (PDPN) Ab and anti- CTL-associated antigen 4 (CTLA-4) Ab in vivo. (A) Evaluation of the tumor volume of AB1-HA tumor-bearing BALB/c mice treated with PMab-1-mG<sub>2a</sub>-f (50 µg per mouse) and/or αCTLA-4 Ab (5 µg per mouse) beginning 7 days after tumor cell injection. (B) Evaluation of the tumor volume of AB1-HA tumor-bearing BALB/c mice treated with PMab-1-mG<sub>2a</sub>-f (50 µg per mouse) and/or programmed death-1 (αPD-1) Ab (100 µg per mouse) beginning 7 days after tumor cell injection. (C–E) Representative images of sections from AB1-HA tumors stained for (C) natural killer (NK) cells, (D) CD8 T cells, and (E) CD4 T cells. Tumors were harvested at day 21 from each group studied in (A). Scale bar, 200 µm. (F–H) Quantitative evaluation of the total number of (F) NK cells, (G) CD8 T cells, and (H) CD4 T cells in the tumors of mice ( $n = 15$  fields per group) is shown in (A). Data are shown as the mean  $\pm$  SEM. \* $p < 0.05$  by a one-way ANOVA.

effect that high concentration Abs interfere with antigen–Ab interactions. Several reports indicated that excessively high concentrations of Abs inhibit ADCC through prozone effects.<sup>41,42</sup> In addition, the prozone-like effect was also reported in animal models.<sup>43</sup> Our preclinical studies indicated that the administration of higher concentration of anti-PDPN Ab could suppress the proper antigen–Ab interactions and ADCC activity. Therefore, we used the low concentration of anti-PDPN Ab in the combined therapy with anti-CTLA-4 Ab.

The present study has several potential clinical implications. First, we revealed the effects of an anti-PDPN Ab on the immune microenvironment of MPM under immunocompetent conditions. Recent studies have shown that the expression of PDPN was detected in 80%–100% of epithelioid MPM patients.<sup>11</sup> Podoplanin expression is known to correlate with a poor prognosis of various solid tumors.<sup>14</sup> Furthermore, several studies have revealed the functional effects of PDPN in promoting tumor invasiveness and metastasis by platelet aggregation.<sup>44–46</sup> Taken together, these findings suggest that novel immunotherapy targeting PDPN is needed, especially in advanced MPMs, considering the insufficient response to current therapies. The present findings could thus enhance the progress made in developing PDPN-targeting therapies for drug discovery. Second, our syngeneic preclinical model enabled the evaluation of combined immunotherapy with anti-PDPN Ab and ICIs. In particular, we identified the potential utility of combined therapy with an anti-PDPN Ab and anti-CTLA-4 Ab as a promising treatment for unresectable MPMs. Finally, the present study indicated the importance of tumor-infiltrating NK cells as key effector cells in immunotherapy.

However, several limitations associated with the present study also warrant mention. First, the efficacy of anti-human PDPN Abs against human MPM in immunocompetent conditions has remained unclear. To address this limitation, a humanized chimera mouse model should be established in future studies. Second, combined immunotherapy with anti-PDPN Ab and anti-CTLA-4 Ab might influence  $T_{reg}$ s. A recent study suggested that some clones of CTLA-4 Abs enhanced the activation of NK cells through the depletion of  $T_{reg}$ s by ADCC.<sup>39</sup> Therefore, in the present study, we used a CTLA-4 blockade clone known to lack ADCC activity on  $T_{reg}$ s.<sup>29</sup> Consistent with the reported study, CTLA-4 Ab increased the tumor-infiltrating  $T_{reg}$ s in our preclinical model, whereas the combined immunotherapy with anti-PDPN Ab and anti-CTLA-4 Ab showed significant antitumor effects. A recent study indicated that the clinically approved anti-CTLA4 Ab ipilimumab has ADCC activity and depletes tumor-infiltrating  $T_{reg}$ s.<sup>47</sup> We therefore considered ipilimumab to have the

potential to demonstrate superior synergistic effects with anti-PDPN Abs through the multiple effects of immune cells, including the activation of NK cells and the depletion of  $T_{reg}$ s.

In summary, we discovered a novel promising treatment by combining immunotherapy with an anti-PDPN Ab and anti-CTLA-4 Ab. The present study identified the pivotal role of NK cells in novel combined immunotherapy targeting PDPN. These findings shed light on the therapeutic strategy for unresectable MPM.

## AUTHOR CONTRIBUTIONS

**Hiroto Yoneda:** Data curation; formal analysis; funding acquisition; investigation; methodology; visualization; writing – original draft.

**Atsushi Mitsuhashi:** Data curation; formal analysis; investigation; methodology; project administration; validation; visualization; writing – review and editing. **Aito Yoshida:** Data curation; formal analysis; investigation; validation; visualization; writing – review and editing.

**Hirokazu Ogino:** Data curation; formal analysis; investigation; methodology; validation; writing – review and editing. **Satoshi Itakura:**

Data curation; formal analysis; investigation; validation; writing – review and editing. **Na Thi Nguyen:** Data curation; formal analysis; investigation; validation; writing – review and editing. **Hiroshi**

**Nokihara:** Data curation; formal analysis; project administration; writing – review and editing. **Seidai Sato:** Data curation; formal analysis; writing – review and editing. **Tsutomu Shinohara:** Supervision;

validation; writing – review and editing. **Masaki Hanibuchi:** Data curation; formal analysis; project administration; validation; writing – review and editing. **Shinji Abe:** Data curation; formal analysis; funding acquisition; investigation; methodology; project administration;

writing – review and editing. **Mika K. Kaneko:** Resources; supervision; writing – review and editing. **Yukinari Kato:** Conceptualization; resources; supervision; writing – review and editing. **Yasuhiko**

**Nishioka:** Conceptualization; data curation; formal analysis; funding acquisition; methodology; project administration; visualization; writing – review and editing.

**ACKNOWLEDGMENTS**  
We thank our colleagues at The University of Tokushima, especially A. Tanabe and R. Akutagawa for their technical assistance. This study was supported by the Support Center for Advanced Medical Sciences, Tokushima University Graduate School of Biomedical Sciences. This research was supported by the Research Support Project for Life Science and Drug Discovery (Basis for Supporting Innovative Drug Discovery and Life Science Research [BINDS]) from AMED under Grant Number JP23ama121008.

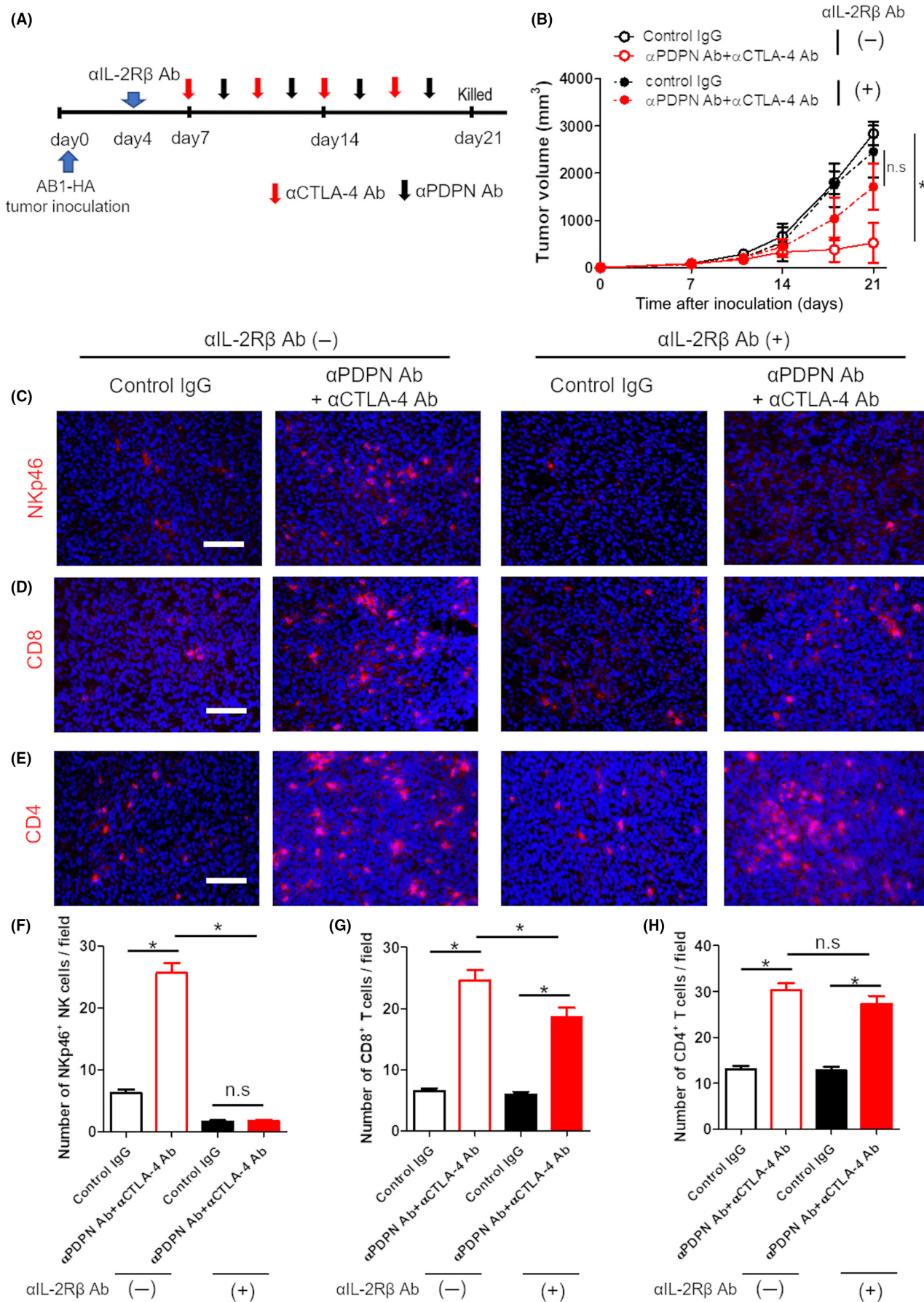


**FIGURE 4** Role of natural killer (NK) cells in combined immunotherapy with antipodoplanin (PDPN) Ab and anti-CTL-associated antigen 4 (CTLA-4) Ab. (A) Treatment schedule of combined therapy with PMab-1-mG<sub>2a</sub>-f (50 µg per mouse) and/or αCTLA-4 Ab (5 µg per mouse) in AB1-HA-bearing mice with the depletion of NK cells by anti-interleukin-2 receptor β-chain (IL-2Rβ) Ab. (B) Evaluation of the tumor volume of AB1-HA tumor-bearing BALB/c mice treated with PMab-1-mG<sub>2a</sub>-f (50 µg per mouse) and αCTLA-4 Ab (5 µg per mouse) beginning 7 days after tumor cell injection with or without the depletion of NK cells. (C–E) Representative images of sections from AB1-HA tumors stained for (E) NK cells, (D) CD8 T cells, and (E) CD4 T cells. Tumors were harvested at day 21 from each group studied in (B). Scale bar, 200 µm. (F–H) Quantitative evaluation of the total number of (F) NK cells, (G) CD8 T cells, and (H) CD4 T cells in the tumors of mice (*n* = 15 fields per group) is shown in (B). Data are shown as the mean ± SEM. \**p* < 0.05 by a one-way ANOVA.

## FUNDING INFORMATION

This study was partly supported by a grant from JSPS KAKENHI Grant Number 19H03668, a Grant-in-Aid for Scientific Research (B) from Japan Society for the Promotion of Science (JSPS) (Y.N.), SPS KAKENHI Grant Number 20K07197, a Grant-in-Aid for Scientific Research (C) from JSPS (S.A.), SPS KAKENHI Grant Number 20K17216, a Grant-in-Aid for Early-Career Scientists from JSPS (H.Y.), and from the Japan Agency for Medical Research and Development (AMED) under Grant Numbers JP22ama121008 (Y.K.) and JP21am0101078 (Y.K.).

## CONFLICT OF INTEREST STATEMENT

All authors declare no conflict of interest.

## ETHICS STATEMENT

Approval of the research protocol by an institutional review board: N/A.

Informed consent: N/A.

Registry and the registration no. of the study/trial: N/A.

Animal studies: All experimental protocols were reviewed and approved by the animal research committee of The University of Tokushima, Japan (approval number T30-130).

## ORCID

Yukinari Kato  <https://orcid.org/0000-0001-5385-8201>

Yasuhiko Nishioka  <https://orcid.org/0000-0001-6311-1654>

## REFERENCES

- Carbone M, Adusumilli PS, Alexander HR, et al. Mesothelioma: scientific clues for prevention, diagnosis, and therapy. *CA Cancer J Clin*. 2019;69:402-429.
- Mutti L, Peikert T, Robinson BWS, et al. Scientific advances and new Frontiers in mesothelioma therapeutics. *J Thorac Oncol*. 2018;13:1269-1283.
- Scherpereel A, Wallyn F, Albelda SM, Munck C. Novel therapies for malignant pleural mesothelioma. *Lancet Oncol*. 2018;19:e161-e172.
- Vogelzang NJ, Rusthoven JJ, Symanowski J, et al. Phase III study of pemetrexed in combination with cisplatin versus cisplatin alone in patients with malignant pleural mesothelioma. *J Clin Oncol*. 2003;21:2636-2644.
- Ribas A, Wolchok JD. Cancer immunotherapy using checkpoint blockade. *Science*. 2018;359:1350-1355.
- Huang AC, Zappasodi R. A decade of checkpoint blockade immunotherapy in melanoma: understanding the molecular basis for immune sensitivity and resistance. *Nat Immunol*. 2022;23:660-670.
- Ceresoli GL, Mantovani A. Immune checkpoint inhibitors in malignant pleural mesothelioma. *Lancet Oncol*. 2017;18:559-561.
- Baas P, Scherpereel A, Nowak AK, et al. First-line nivolumab plus ipilimumab in unresectable malignant pleural mesothelioma (CheckMate 743): a multicentre, randomised, open-label, phase 3 trial. *Lancet*. 2021;397:375-386.
- Breiteneder-Geleff S, Matsui K, Soleiman A, et al. Podoplanin, novel 43-kd membrane protein of glomerular epithelial cells, is down-regulated in puromycin nephrosis. *Am J Pathol*. 1997;151:1141-1152.
- Breiteneder-Geleff S, Soleiman A, Kowalski H, et al. Angiosarcomas express mixed endothelial phenotypes of blood and lymphatic capillaries: podoplanin as a specific marker for lymphatic endothelium. *Am J Pathol*. 1999;154:385-394.
- Ordóñez NG. D2-40 and podoplanin are highly specific and sensitive immunohistochemical markers of epithelioid malignant mesothelioma. *Hum Pathol*. 2005;36:372-380.
- Kato Y, Fujita N, Kunita A, et al. Molecular identification of Aggrus/T1alpha as a platelet aggregation-inducing factor expressed in colorectal tumors. *J Biol Chem*. 2003;278:51599-51605.
- Kato Y, Kaneko M, Sata M, Fujita N, Tsuruo T, Osawa M. Enhanced expression of Aggrus (T1alpha/podoplanin), a platelet-aggregation-inducing factor in lung squamous cell carcinoma. *Tumour Biol*. 2005;26:195-200.
- Krishnan H, Rayes J, Miyashita T, et al. Podoplanin: an emerging cancer biomarker and therapeutic target. *Cancer Sci*. 2018;109:1292-1299.
- Jiang XR, Song A, Bergelson S, et al. Advances in the assessment and control of the effector functions of therapeutic antibodies. *Nat Rev Drug Discov*. 2011;10:101-111.
- Musolino A, Gradishar WJ, Rugo HS, et al. Role of Fcγ receptors in HER2-targeted breast cancer therapy. *J Immunother Cancer*. 2022;10:e003171.
- Coleman N, Yap TA, Heymach JV, Meric-Bernstam F, le X. Antibody-drug conjugates in lung cancer: dawn of a new era? *NPJ Precis Oncol*. 2023;7:5.
- Kato Y, Kaneko MK, Kunita A, et al. Molecular analysis of the pathophysiological binding of the platelet aggregation-inducing factor podoplanin to the C-type lectin-like receptor CLEC-2. *Cancer Sci*. 2008;99:54-61.
- Kaneko MK, Kunita A, Abe S, et al. Chimeric anti-podoplanin antibody suppresses tumor metastasis through neutralization and antibody-dependent cellular cytotoxicity. *Cancer Sci*. 2012;103:1913-1919.
- Abe S, Kaneko MK, Tsuchihashi Y, et al. Antitumor effect of novel anti-podoplanin antibody NZ-12 against malignant pleural mesothelioma in an orthotopic xenograft model. *Cancer Sci*. 2016;107:1198-1205.
- Kaji C, Tsujimoto Y, Kato Kaneko M, Kato Y, Sawa Y. Immunohistochemical examination of novel rat monoclonal antibodies against mouse and human Podoplanin. *Acta Histochem Cytochem*. 2012;45:227-237.



22. Kaneko MK, Ohishi T, Takei J, et al. Anti-EpCAM monoclonal antibody exerts antitumor activity against oral squamous cell carcinomas. *Oncol Rep*. 2020;44:2517-2526.
23. Niwa R, Shoji-Hosaka E, Sakurada M, et al. Defucosylated chimeric anti-CC chemokine receptor 4 IgG1 with enhanced antibody-dependent cellular cytotoxicity shows potent therapeutic activity to T-cell leukemia and lymphoma. *Cancer Res*. 2004;64:2127-2133.
24. Kaneko MK, Ohishi T, Nakamura T, et al. Development of Core-Fucose-deficient humanized and chimeric anti-human Podoplanin antibodies. *Monoclon Antib Immunodiagn Immunother*. 2020;39:167-174.
25. Oyewole-Said D, Konduri V, Vazquez-Perez J, Weldon SA, Levitt JM, Decker WK. Beyond T-cells: functional characterization of CTLA-4 expression in immune and non-immune cell types. *Front Immunol*. 2020;11:608024.
26. Walker LS, Sansom DM. Confusing signals: recent progress in CTLA-4 biology. *Trends Immunol*. 2015;36:63-70.
27. Tanaka T, Kitamura F, Nagasaka Y, Kuida K, Suwa H, Miyasaka M. Selective long-term elimination of natural killer cells in vivo by an anti-interleukin-2 receptor  $\beta$  chain monoclonal antibody in mice. *J Exp Med*. 1993;178:1103-1107.
28. Yano S, Nishioka Y, Izumi K, et al. Novel metastasis model of human lung cancer in SCID mice depleted of NK cells. *Int J Cancer*. 1996;67:211-217.
29. Marangoni F, Zhakyp A, Corsini M, et al. Expansion of tumor-associated Treg cells upon disruption of a CTLA-4-dependent feedback loop. *Cell*. 2021;184:3998-4015.
30. Simpson TR, Li F, Montalvo-Ortiz W, et al. Fc-dependent depletion of tumor-infiltrating regulatory T cells co-defines the efficacy of anti-CTLA-4 therapy against melanoma. *J Exp Med*. 2013;210:1695-1710.
31. Sharma A, Subudhi SK, Blando J, et al. Anti-CTLA-4 immunotherapy does not deplete FOXP3<sup>+</sup> regulatory T cells (T<sub>reg</sub>s) in human cancers. *Clin Cancer Res*. 2019;25:1233-1238.
32. Chinen T, Kannan AK, Levine AG, et al. An essential role for the IL-2 receptor in Treg cell function. *Nat Immunol*. 2016;17:1322-1333.
33. Jin WJ, Erbe AK, Schwarz CN, et al. Tumor-specific antibody, Cetuximab, enhances the in situ vaccine effect of radiation in immunologically cold head and neck squamous cell carcinoma. *Front Immunol*. 2020;11:591139.
34. Ramamoorthi G, Kodumudi K, Snyder C, et al. Intratumoral delivery of dendritic cells plus anti-HER2 therapy triggers both robust systemic antitumor immunity and complete regression in HER2 mammary carcinoma. *J Immunother Cancer*. 2022;10(6):e004841.
35. Cao Y, Wang X, Jin T, et al. Immune checkpoint molecules in natural killer cells as potential targets for cancer immunotherapy. *Signal Transduct Target Ther*. 2020;5:250.
36. Sivori S, Della Chiesa M, Carlomagno S, et al. Inhibitory receptors and checkpoints in human NK cells, implications for the immunotherapy of cancer. *Front Immunol*. 2020;11:2156.
37. Stojanovic A, Fiegler N, Brunner-Weinzierl M, Cerwenka A. CTLA-4 is expressed by activated mouse NK cells and inhibits NK cell IFN- $\gamma$  production in response to mature dendritic cells. *J Immunol*. 2014;192:4184-4191.
38. Davis-Marcisak EF, Fitzgerald AA, Kessler MD, et al. Transfer learning between preclinical models and human tumors identifies a conserved NK cell activation signature in anti-CTLA-4 responsive tumors. *Genome Med*. 2021;1:129.
39. Sanseviero E, O'Brien EM, Karras JR, et al. Anti-CTLA-4 activates Intratumoral NK cells and combined with IL15/IL15R $\alpha$  complexes enhances tumor control. *Cancer Immunol Res*. 2019;7:1371-1380.
40. Wagner AK, Kadri N, Tibbitt C, et al. PD-1 expression on mouse intratumoral NK cells and its effects on NK cell phenotype. *iScience*. 2022;25:105137.
41. Jenkins M, Mills J, Kohl S. Natural killer cytotoxicity and antibody-dependent cellular cytotoxicity of human immunodeficiency virus-infected cells by leukocytes from human neonates and adults. *Pediatr Res*. 1993;33(5):469-474.
42. Mulgrew K, Kinneer K, Yao XT, et al. Direct targeting of alphavbeta3 integrin on tumor cells with a monoclonal antibody, Abegrin. *Mol Cancer Ther*. 2006;5(12):3122-3129.
43. Vaidya KS, Oleksijew A, Tucker LA, et al. A "Prozone-like" effect influences the efficacy of the monoclonal antibody ABT-700 against the hepatocyte growth factor receptor. *Pharmacology*. 2017;100(5-6):229-242.
44. Takeuchi S, Fukuda K, Yamada T, et al. Podoplanin promotes progression of malignant pleural mesothelioma by regulating motility and focus formation. *Cancer Sci*. 2017;108:696-703.
45. Takemoto A, Takagi S, Ukaji T, et al. Targeting Podoplanin for the treatment of osteosarcoma. *Clin Cancer Res*. 2022;28:2633-2645.
46. Kunita A, Kashima TG, Morishita Y, et al. The platelet aggregation-inducing factor aggrus/podoplanin promotes pulmonary metastasis. *Am J Pathol*. 2007;170:1337-1347.
47. Romano E, Kusio-Kobialka M, Foukas PG, et al. Ipilimumab-dependent cell-mediated cytotoxicity of regulatory T cells ex vivo by nonclassical monocytes in melanoma patients. *Proc Natl Acad Sci U S A*. 2015;112:6140-6615.

## SUPPORTING INFORMATION

Additional supporting information can be found online in the Supporting Information section at the end of this article.

**How to cite this article:** Yoneda H, Mitsushashi A, Yoshida A, et al. Antipodoplanin antibody enhances the antitumor effects of CTLA-4 blockade against malignant mesothelioma by natural killer cells. *Cancer Sci*. 2024;115:357-368. doi:[10.1111/cas.16046](https://doi.org/10.1111/cas.16046)